SUPPLEMENTARY FIGURE LEGENDS

Figure S1. Additional characterization of *Atg5VC* colons. (A, B) Colonic sections from control and *Atg5VC* mice fluorescently stained for (A) Muc2 or (B) UEA. Bars=200μm. (C) H&E stained sections of descending colons from control and *Atg5VC* mice. Bars=200μm. (D-G) Quantification of the average (D) crypt height, (E) number of mitotic cells per crypt, (F) number of epithelial apoptotic cells/545 μm of mucosa, and (G) number of neutrophils/545 μm of mucosa counted from H&E stained sections of descending colons from control and *Atg5VC* mice (n=3 mice/group). Error bars represent standard deviations. No statistically significant differences were found in all three measurements as determined by the Student's *t* test.

Figure S2. *Atg7VC* and *LC3B*$^{-/-}$ goblet cell accumulate mucin. (A and C) Alcian blue-stained sections of descending colons from controls and (A) *Atg7VC* (C) *LC3β*$^{-/-}$ mice. Bars=200μm. (B and D) Quantification of average mucin area/goblet cell in control, *Atg7VC, and LC3β*$^{-/-}$ mice (n=5-7 mice/group from 3 independent experiments; 100 goblet cells measured/ mouse). ***, P<0.001 as determined by the Student's *t* test.

Figure S3. Tat-Cre treatment of *FIP200*$^{f/f}$ and *Atg14*$^{f/f}$ organoids. (A) Representative images of a single colonic spheroid cultured in either 50% conditioned media (CM) or 5% CM + 5μM DAPT. (B-C) Genotyping results of *Atg14*$^{f/f}$ and *FIP200*$^{f/f}$ spheroid clones treated with recombinant Tat-cre.

Figure S4. LC3 localizes to multi-vesicular vacuoles. Lower power Immunogold TEM image for LC3β from a wild-type mouse shown in Figure 3B. LC3-positive vacuole is marked within the white dashed box. MG: mucin granule

Figure S5. Microarray analysis of Atg5-deficient colonic epithelium reveals defects in endocytosis but not mucin production. (A) KEGG pathway schematic generated from DAVID bioinformatics suite. Red stars indicate genes (in the green boxes) whose mRNA levels were different between control and Atg5-deficient colonic crypt base epithelial cells. Green Arrows indicate molecular interaction or relation (B) Table of genes that have differential expression in Atg5-deficient crypt base epithelial cells that are part of the KEGG endocytosis pathway. (C) A heat map of the highest ranking Gene Ontology FAT terms (determined using the DAVID bioinformatics program) under the cellular component domain for Atg5-deficient epithelial cells obtained from a microarray comparing control and *Atg5VC* colonic crypt base epithelium. The color scale corresponds to the number of genes pertaining to the GO term for *Atg5VC* mice. The significance of enrichment was calculated using a modified Fisher's exact test. (D) Expression ratio (comparing Atg5-deficient colonic epithelium to control) of the major secreted mucins in the colon.

Figure S6. Inhibition of clathrin-mediated endocytosis results in goblet cell mucin accumulation. (A) Images of wild-type colonic epithelial organoids labeled with TRITC-UEA (red) after treatment with vehicle, negative control, or 100μM Pitstop2. Bars=20μm. (B) Quantification of average mucin area/goblet cell (n=3 independent experiments/group; each experiment with two replicate wells; 30-90 cells were quantified/well). Error bars indicate SEM. ****, $P<0.0001$ as determined by ANOVA with Tukey's multiple post-test comparisons.

Figure S7. NADPH oxidase deficiency results in goblet cell mucin accumulation. (A) p22phox immunoblot of colonic spheroids treated with 100nm BafA1 as indicated (B) Low power immunogold TEM image for LCβ and p22phox shown in Figure 5E (C) Semi-quantitative PCR results showing p47phox expression in the spleen and colonic organoids. (C-E) Periodic

Acid-Schiff/Alcian Blue stained sections of descending colons from (D) control and *p47phox*$^{-/-}$ and control and mice treated with 3% NAC in the drinking water. Bars=200μm. (E) Quantification of average mucin area/goblet cell in control and *p47phox*$^{-/-}$ mice (n=5-7 mice/group from 3 independent experiments; 100 goblet cells measured/ mouse). **, P<0.01 as determined by the Student's *t* test.

Figure S8. Loss of ROS results in goblet cell mucin accumulation. Periodic Acid-Schiff/Alcian Blue stained sections of descending colons from control mice treated with 3% NAC in the drinking water. Bars=200μm.

Figure S9. ROS mediated intracellular calcium release is important for goblet cell function. (A) LC3 immunoblots of colonic spheroids treated with 300 μM hydrogen peroxide or 100nm BafA1 as indicated. Representative image is shown from n=3 experiments. (B) Quantification of intracellular calcium using Fluo-4 in wild-type colonic spheroids treated with BAPTA-AM, Atg5VC and p22 mut spheroids treated with or without ionomycin. All measurements are relative to untreated controls (n=3 experiments). Error bars indicate SEM. (C-D) LC3 immunoblots of colonic spheroids treated with 100 μM BAPTA, 100 nM ionomycin, or 100 nM BafA1 as indicated.

Figure S1

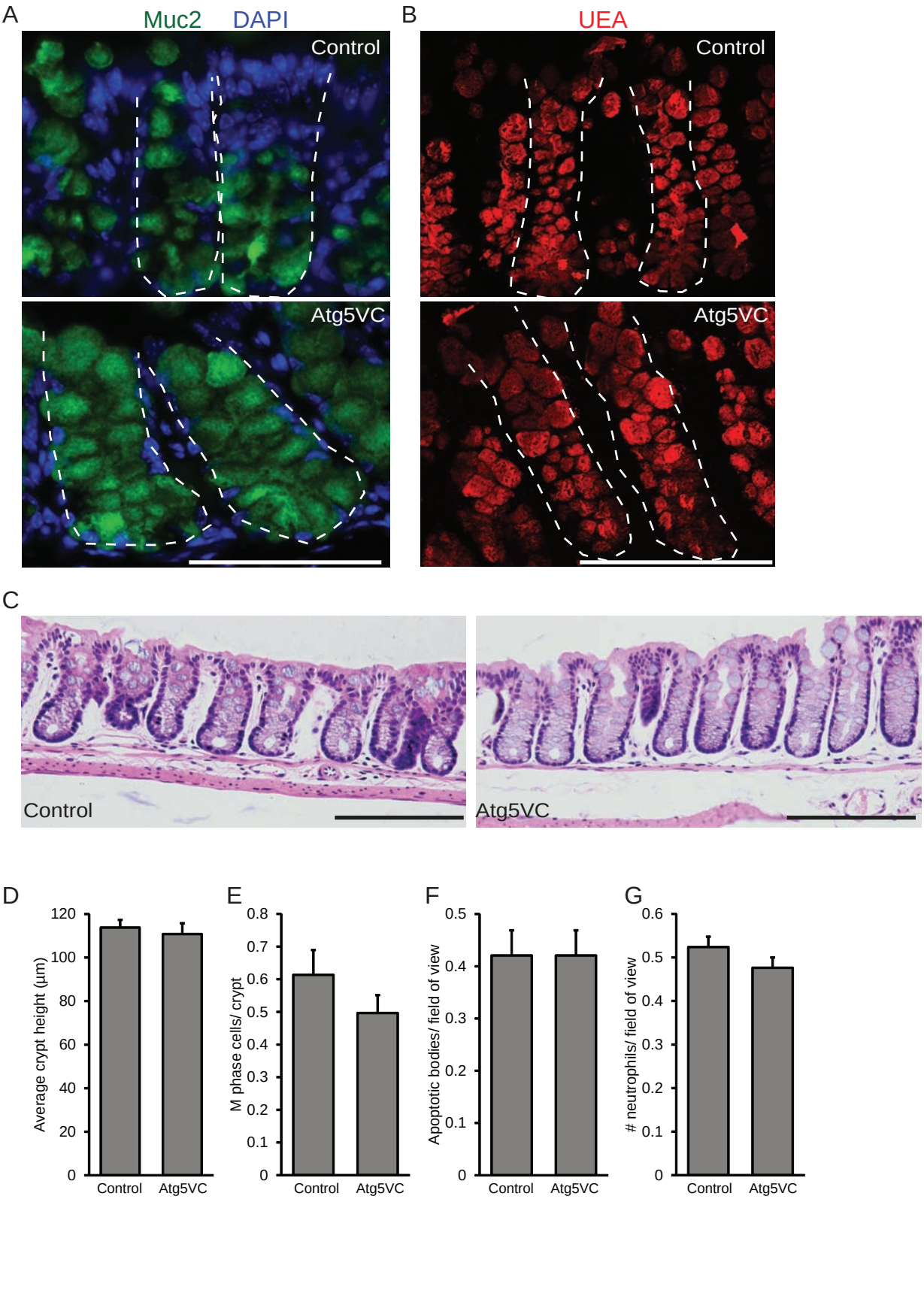
A
Muc2
DAPI
Control
Atg5VC
B
UEA
Control
Atg5VC
C
Control
Atg5VC
D
Average crypt height (μm)
120
100
80
60
40
20
0
Control
Atg5VC
E
M phase cells/ crypt
0.8
0.7
0.6
0.5
0.4
0.3
0.2
0.1
0
Control
Atg5VC
F
Apoptotic bodies/ field of view
0.5
0.4
0.3
0.2
0.1
0
Control
Atg5VC
G
neutrophils/ field of view
0.6
0.5
0.4
0.3
0.2
0.1
0
Control
Atg5VC

Figure S2

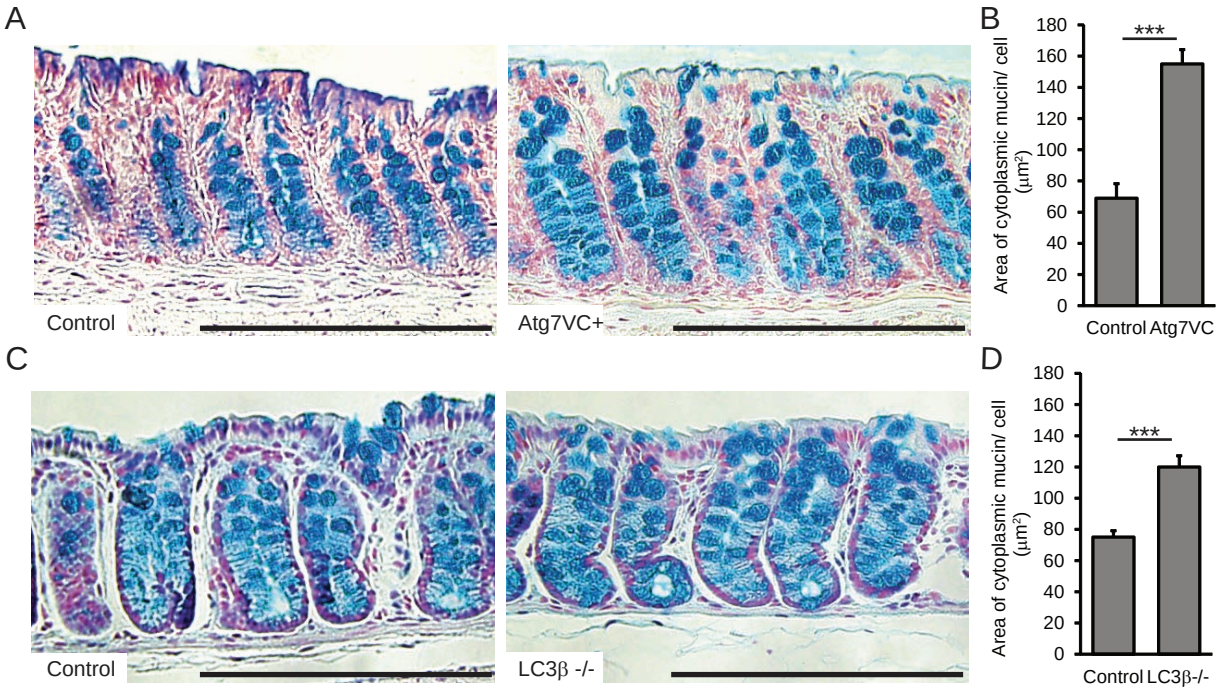
A
Control
Atg7VC+
B
Area of cytoplasmic mucin/ cell (μm²)
180
160
140
120
100
80
60
40
20
0
***
Control
Atg7VC
C
Control
LC3β -/-
D
Area of cytoplasmic mucin/ cell (μm²)
180
160
140
120
100
80
60
40
20
0
***
Control
LC3β-/-

Figure S3

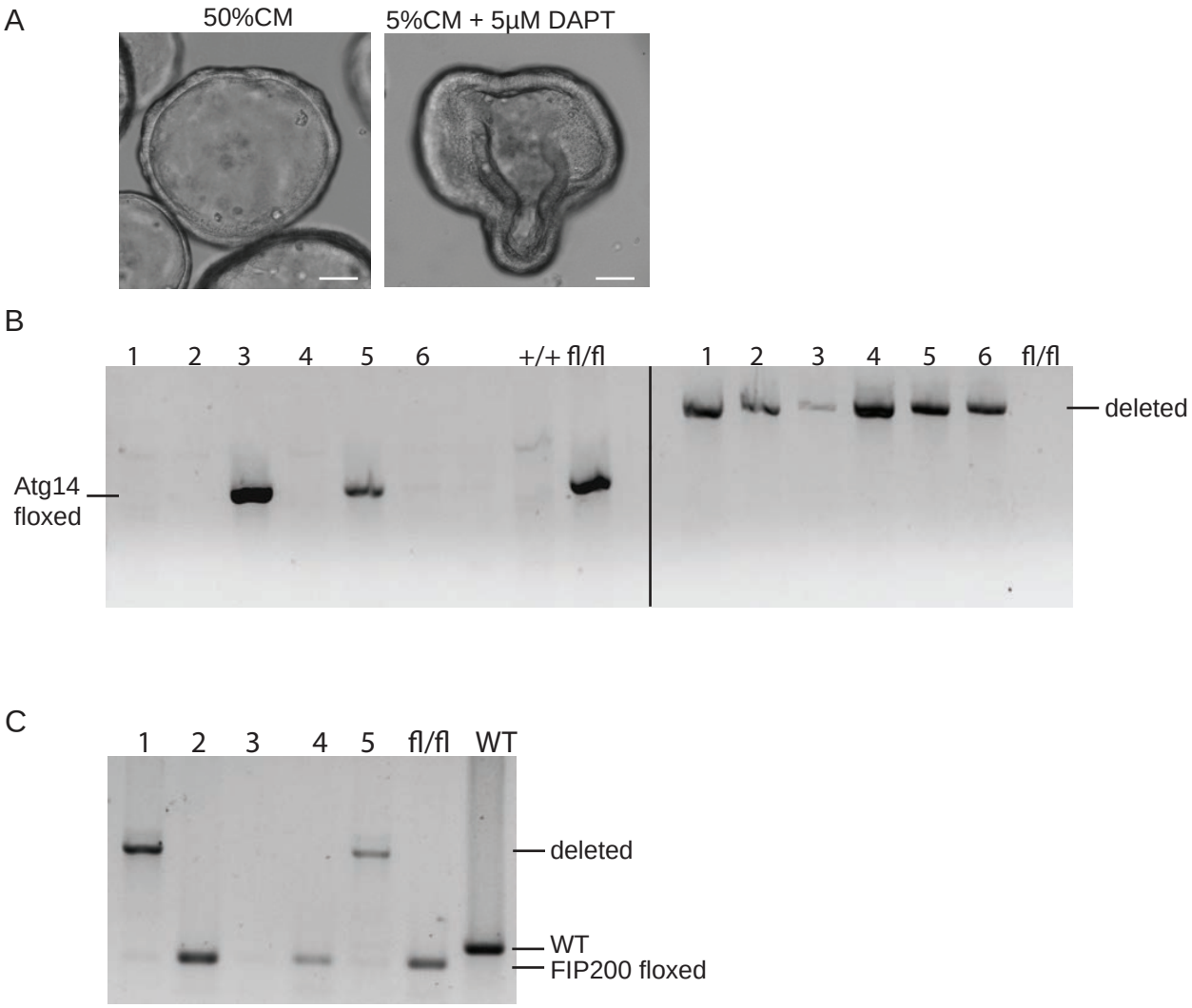
A
50%CM
5%CM + 5μM DAPT
B
1 2 3 4 5 6 +/+ fl/fl
1 2 3 4 5 6 fl/fl
Atg14
floxed
deleted
C
1 2 3 4 5 fl/fl WT
deleted
WT
FIP200 floxed

Figure S4

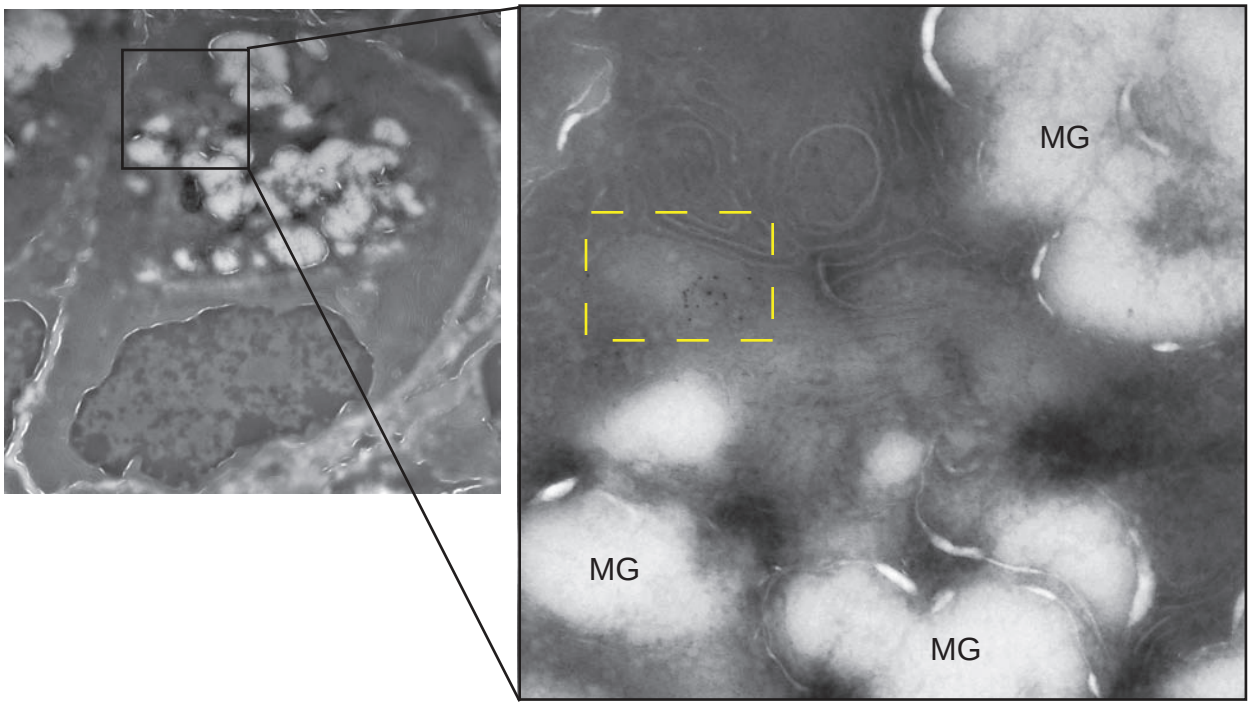

Figure S5

A

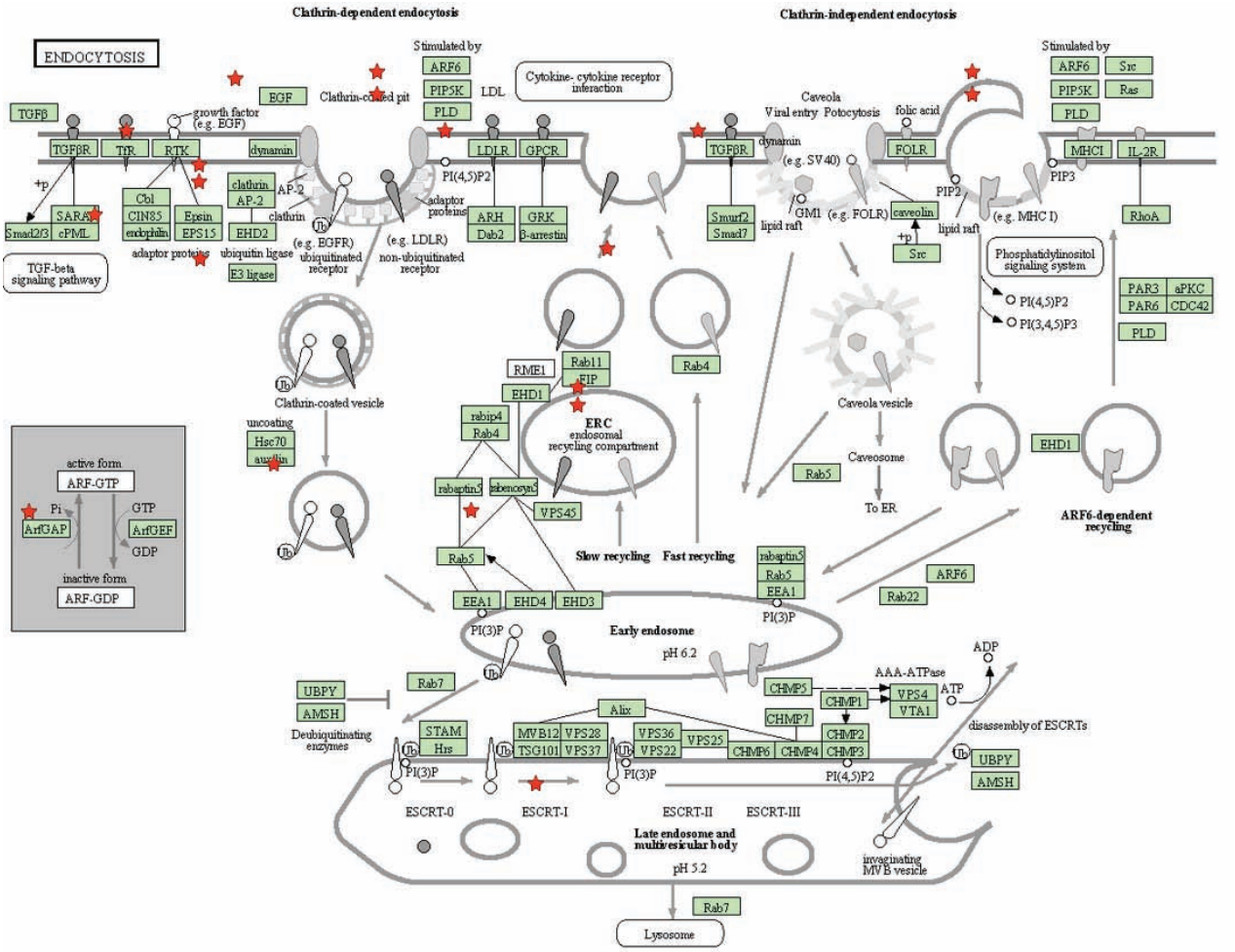

B

Gene	Fold change
RAB11B	2.050263
RET	1.695945
VPS28	1.683376
RAB11FIP1	1.666225
H2-K1	1.647814
KIT	1.647683
PIP4K2B	1.628006
PLD1	1.599904
CLTC	1.519121
IGF1R	1.515073
AP2A2	-1.504144
KDR	-1.549085
PIP5K1B	-1.549547
EGF	-1.644696
ZFYVE20	-1.679264
LDLR	-1.748821
SH3GLB1	-1.824857

C

GO term CC	*P*-value
Golgi Apparatus	4.1E-03
Endomembrane System	1.2E-03
Cell Fraction	1.4E-02
Cell Projection	2.8E-02
Insoluble Fraction	2.0E-02
Membrane Fraction	1.9E-02
Internal Side Of Plasma Membrane	9.1E-03
Cell Surface	3.2E-02
Endosome	2.5E-02
Actin Cytoskeleton	4.2E-02
Anchoring Junction	1.2E-02
Ruffle	3.5E-02

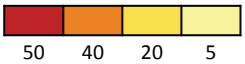

D

Secreted Mucin	Expression Ratio (Atg5VC: control)
Muc2	0.85
Muc5AC	0.96
Muc6	1.02

Figure S6

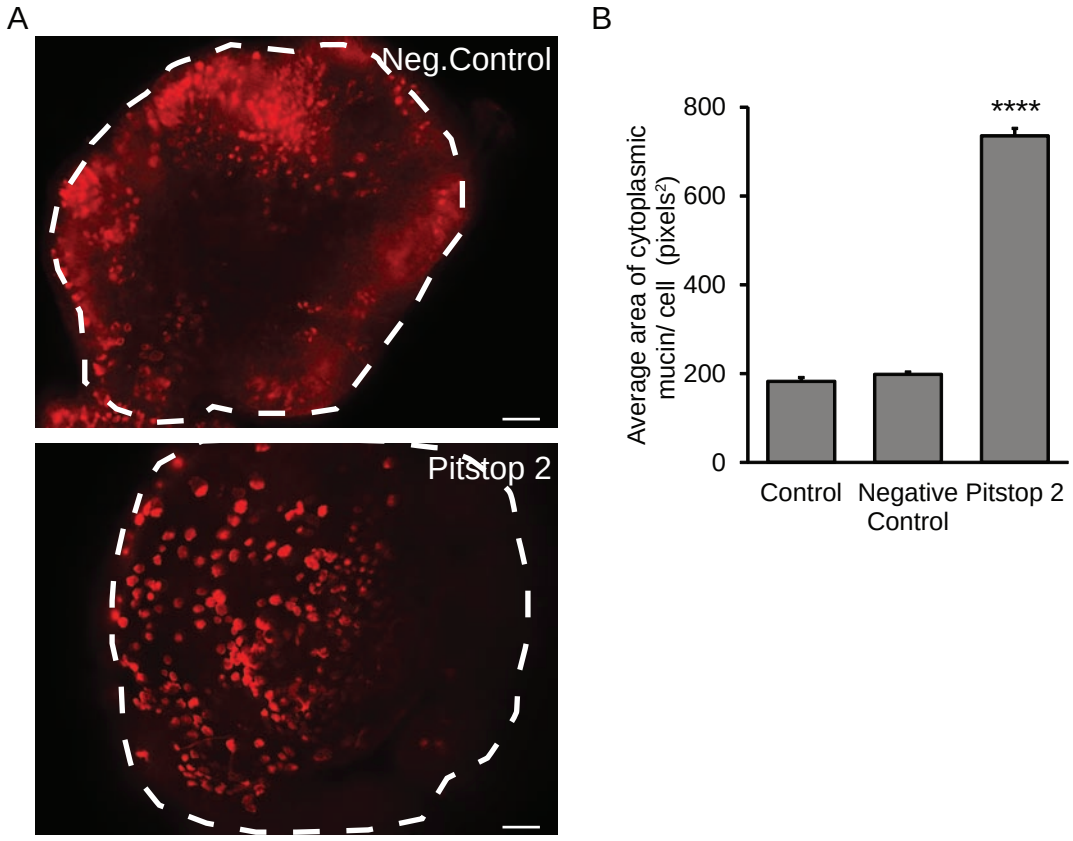
A
Neg.Control
Pitstop 2
B
Average area of cytoplasmic mucin/ cell (pixels²)
800
600
400
200
0
****
Control
Negative Control
Pitstop 2

Figure S7

A

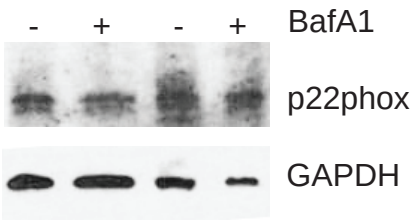

B

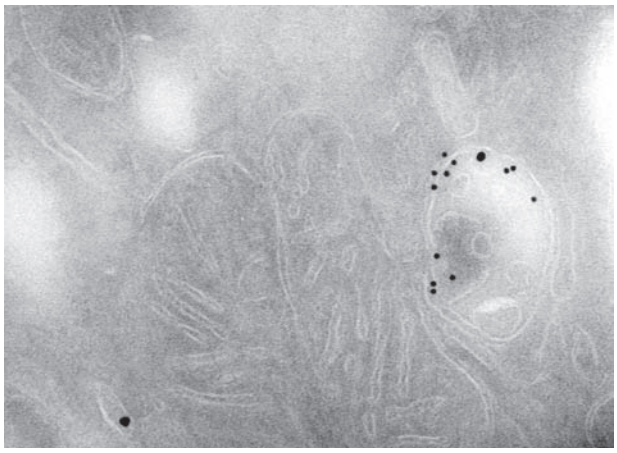

C

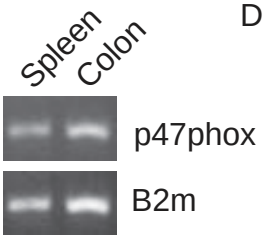

D

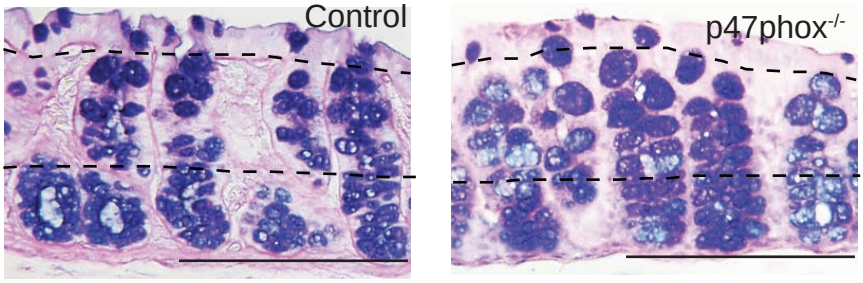

E

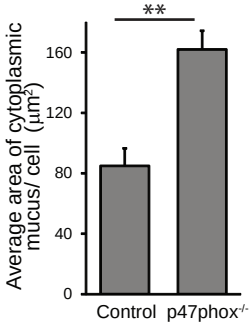

Figure S8

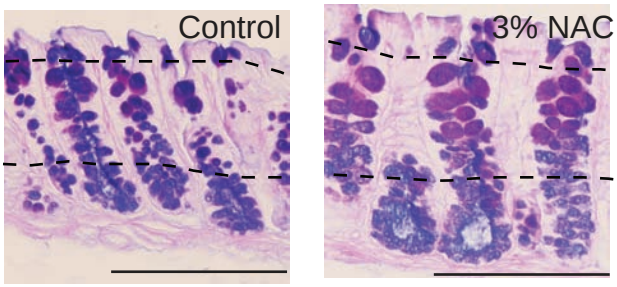

Figure S9

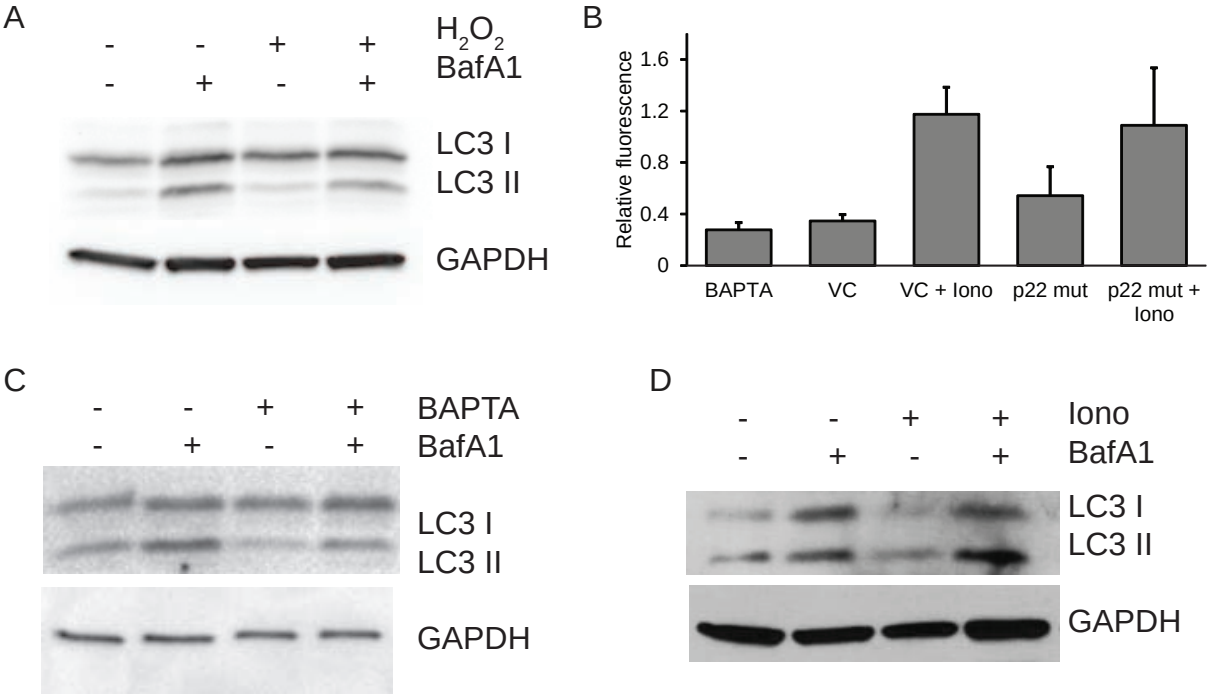
A
- - + + H_2O_2
- + - + BafA1
LC3 I
LC3 II
GAPDH
B
Relative fluorescence
1.6
1.2
0.8
0.4
0
BAPTA
VC
VC + Iono
p22 mut
p22 mut + Iono
C
- - + + BAPTA
- + - + BafA1
LC3 I
LC3 II
GAPDH
D
- - + + Iono
- + - + BafA1
LC3 I
LC3 II
GAPDH